# Superradiant emission from a degenerate medium

J. A. Hermann
*Materials Research Laboratories, Defence Science and Technology Organisation, Ascot Vale, Victoria 3032, Australia*
(Received 21 March 1984; revised manuscript received 27 December 1984)

The emission of radiation from a spatially extended amplifying medium is shown to exhibit new coherence effects when the medium is modeled by inverted atoms which possess a degeneracy allowing $Q(J)$ transitions. In particular, it is predicted that media of this type for which $J=2$ can emit leading pulses which are doubly peaked or asymmetric within both the regimes of superfluorescence and oscillating fluorescence. Dissipative processes can radically alter the character of the emission; an output consisting of two well-separated pulses appears feasible, but the precise behavior in the present model depends upon the magnitude of the field losses and the initiation statistics.

## I. INTRODUCTION

A number of effects appearing in the phenomenon of self-induced transparency (SIT) have been attributed to the presence of degeneracies. A degenerate transition generally can occur when several different two-level transitions interact via a common radiation field in a cooperative manner. Such processes can be "accidental," but are more often associated with the selection rules for an atomic transition (e.g., as in $F=2\rightarrow F'=2$ hyperfine degeneracies) or with a vibration-rotation transition in a molecule. The coherent effects associated with the presence of these degeneracies in an attenuating medium have been extensively investigated both theoretically and experimentally;[1–12] however, little attention has been directed to their presence in *amplifying* situations hitherto, apart from brief treatments of their expected consequences in superfluorescence (SF)[13] and in swept-gain amplification.[14]

In this paper attention will be directed to the problem of cooperative emission from an initially inverted and spatially extended medium which will be modeled by a collection of degenerate atoms allowing only the so-called $Q(J)$ transitions. Transitions with this symmetry possess dipole matrix elements whose ratios are integers, which leads to some interesting consequences. Our model requires that the atoms be sufficiently close for cooperative effects to occur and also that the active medium, assumed to take the form of a rod of length $L$, be less than a certain "cooperation length" $L_c=c(\frac{1}{2}\tau_R\tau_E)^{1/2}$ [$\tau_E=2Lc^{-1}$ is the round-trip time, and $\tau_R=(2\pi\mu^2 n\omega_0 L\hbar^{-1}c^{-1})^{-1}$ is the superradiance time; $\omega_0$ is the atomic frequency, $n$ is the atomic number density, and the various dipole matrix elements are whole fractions of $\mu$]. In common with previous semiclassical treatments of SIT (Refs. 1–5 and 12) and of SF (Refs. 15–24) it will be supposed that inhomogeneous broadening is absent and the resonance is exact and furthermore that both the electric field and the macroscopic polarization may be described in the slowly-varying-envelope and rotating-wave approximations, so that the effects of the higher harmonics can be neglected.

The semiclassical equations coupling the field and atomic variables in the theory of the two-way emission process from a rodlike medium of two-level atoms have been derived from a two-mode ansatz by Saunders *et al.*[20] and suffice to describe the essentials of superradiant emission. Transverse spatial effects have been neglected, and field losses have been simulated by incorporating a linear loss term in the field amplitude equation. It has been shown[16,17,25,26] that once a macroscopic dipole is established, the influence of quantum and semiclassical noise upon the dynamics is minimal and that the subsequent processes are well described semiclassically. The derivation of the two-way Maxwell-Bloch equations as in Ref. 20 is readily extended to take into account the $J$-fold set of polarization variables for a $Q(J)$ degeneracy, leading to the following equations of motion:

$$\frac{\partial E^{\pm}}{\partial T}\pm\frac{\partial E^{\pm}}{\partial X}+\kappa L E^{\pm}=\alpha\sum_{i=1}^{J}p_i\lambda_i P_i^{\pm}\ , \tag{1a}$$

$$\frac{\partial P_i^{\pm}}{\partial T}=p_i E^{\pm}N_i-\tfrac{1}{2}\tau_E\gamma_2 P_i^{\pm}\ , \tag{1b}$$

$$\frac{\partial N_i}{\partial T}=-p_i(E^{+}P_i^{-}+E^{-}P_i^{-})-\tau_E\gamma_1(1+N_i)\ , \tag{1c}$$

where $E^{\pm}(X,T)$ are the amplitudes of the oppositely directed field envelopes, $P_i^{\pm}(X,T)$ are the corresponding components of the macroscopic polarization, and $N_i(X,T)$ are the inversions ($X=x/L$ and $T=ct/L$ are suitably scaled space and time coordinates); a parameter of crucial importance is $\alpha=\frac{1}{2}\tau_E\tau_R^{-1}$, and the dipole matrix ratios are $p_i=i/J$, while the fractional numbers $\lambda_i$ are the weightings of each species of dipole initially. The homogeneous lifetimes of the atoms are $\gamma_2^{-1}$ and $\gamma_1^{-1}$. Linear damping of the amplitudes has been allowed for, but phase effects have been disregarded.

A systematic investigation of Eqs. (1a)–(1c) was undertaken by numerical computation. The $J=2$ system, being the simplest case, was chosen for extensive study in an attempt to gain understanding of the physics as well as the roles of the various parameters. Initiation of the radiant emission was simulated by introducing tipping angles for the collective Bloch vectors associated with each degenerate component, in line with some previous practice with

 

simpler systems.[21–24] This can be justified if the mechanism of the initiation process is considered to be subordinate to the dynamics of the subsequent emission. Thus, the important effects accompanying the degeneracy only show up in the regime of *nonlinear* behavior. Essential initial conditions in a semiclassical approach are

$$E^{\pm}(X,0)=0, \quad 1-N_i(X,0)=\Delta_i>0 \tag{2}$$

while the boundary conditions are correspondingly

$$E^{+}(0,T)=E^{-}(1,T)=0 \ . \tag{3}$$

As in the nondegenerate case, the magnitude of the parameter $\alpha$ determines whether the emission is superradiant ($\alpha \ll 1$, $E^{\pm} \propto n$) or steadily oscillating ($\alpha \gg 1$, $E^{\pm} \propto n^{1/2}$) or somewhere between these two extremes. With a two-way process, and ignoring atomic losses, we find from Eqs. (1a)—(1c) the constants of motion

$$N_i^2+(P_i^{+})^2+(P_i^{-})^2=1, \ i=1,2,\ldots,J \ . \tag{4}$$

It therefore seems permissible to define two sets of "angles" $\sigma_i(X,T)$ and $\rho_i(X,T)$ by the relations

$$N_i=\cos\sigma_i, \quad P_i^{\pm}=\sin\sigma_i \times \begin{cases} \sin\rho_i \\ \cos\rho_i \end{cases} . \tag{5}$$

The various Bloch angles $\sigma_i$, although different, are usually related to each other in SIT in a simple way. Thus for SIT there is effective a single collective Bloch angle. This is not necessarily true in SF emission with the identical degeneracies. In this model we have chosen the initial conditions in Eq. (2) such that $\Delta_1=\Delta_2=\cdots=\Delta_J(=\Delta)$ and will assume that $\Delta$ is independent of $X$ throughout the medium. The initial polarization envelopes are roughly proportional to the tipping angles $\sigma_i(X,0)\simeq(2\Delta)^{1/2}$. Since $\rho_i=\tan^{-1}(P_i^{+}/P_i^{-})$, the initial value for all $\rho_i$ is $\pi/4$. When $P_i^{+} \gg P_i^{-}$ we expect that $\rho_i \simeq \pi/2$, and for $P_i^{+} \ll P_i^{-}$ we expect $\rho_i \simeq 0$.

## II. INITIAL DEVELOPMENT

It is appropriate to discuss, and to justify the selection of, the tipping angles used to initiate the evolution of the collective Bloch vectors. This is particularly important when an attempt is made to simulate superradiant emission initiated by quantum fluctuations, i.e., superfluorescence. Even where the initial state of an inverted system has been carefully prepared (e.g., by injecting a coherent pulse of known area at the transition wavelength immediately following inversion), random fluctuations may still occur and need to be accounted for. The result of these processes is that radiant emissions from apparently identically prepared samples may fluctuate significantly in shape from shot to shot.

In the case of SF a common physical interpretation of the tipping angle is that it simulates the effect of fluctuations upon the average (mean-squared) Bloch angle, where the averaging refers to many repeated experiments. Some authors[27–29] have identified the fluctuations with an initial uncertainty in the atomic polarization, while other authors[30–34] have identified them as zero-point fluctuations of the initial vacuum field. These approaches correspond to different mathematical techniques and are physically equivalent. There is also an apparently semiclassical interpretation of the initial tipping angle in SF.[16–19]

Regardless of the interpretation, Vrehen and Schuurmans have directly measured[34] an effective initial tipping angle in SF. In their experiment a small-area coherent pulse at the SF wavelength was injected into a sample of newly inverted cesium atoms. Both the delay and shape of the output pulse were measured as functions of the area. When the area exceeded a certain threshold, the delay time was reduced. This threshold area agrees with a value for the effective tipping angle of order $2/\sqrt{N}$ ($N$ being the number of initially inverted atoms) as predicted by theories of SF which allow for both quantum fluctuations and propagation effects.

For SF with degenerate media, it may be assumed that indirect inversion of the transitions of interest can be carried out simultaneously. The additional assumption that the tipping angles required to initiate the evolution are dependent only upon $N$ implies [for $Q(J)$ transitions with equal $\lambda_i$ weightings] that these angles possess the same order of magnitude. Also significant are some numerical solutions of Eqs. (1a)—(1c) (see Sec. III) which indicate that a $Q(J)$-degenerate medium, prepared with initial angles $\sigma_i(X,0)$ differing by several orders of magnitude, will evolve essentially like an identical system with each initial set equal to the largest of the above $\sigma_i(X,0)$. This result may be understood by considering a simplified model of the emission which ignores the coupling between counterpropagating waves; the limits of its validity have been set out previously.[21–24] Ignoring polarization losses, we can replace Eqs. (1a)—(1c) with

$$\frac{\partial E}{\partial T}+\frac{\partial E}{\partial X}+\kappa LE=\alpha \sum_{i=1}^{J} p_i\lambda_i P_i \ , \tag{6a}$$

$$\frac{\partial P_i}{\partial T}=p_i E N_i \ , \tag{6b}$$

$$\frac{\partial N_i}{\partial T}=-p_i E P_i \ . \tag{6c}$$

These new equations correspond to setting $E=E^{+}$, $P_i=P_i^{+}$, and $P_i^{-}=0$ in the previous equations. Furthermore, the field amplitude is now simply $E=p_i^{-1}\partial\sigma_i/\partial T$, implying the following conservation identity for any pair of Bloch angles $\sigma_1,\sigma_2$:

$$\frac{\sigma_1(X,T)}{p_1}-\frac{\sigma_2(X,T)}{p_2}=\frac{\sigma_1(X,0)}{p_1}-\frac{\sigma_2(X,0)}{p_2} \ .$$

This identity has the obvious consequence that, whenever $\sigma_i(X,T) \gg \sigma_i(X,0)$,

$$\sigma_1=(p_1/p_2)\sigma_2+O[\sigma_i(X,0)] \ .$$

Hence there are "preferred ratios" between the Bloch angles, which are realized in the long-time evolution of the system.

The transition to a dynamical state in which the Bloch angles are locked together in fixed ratios must occur be-

fore the nonlinear behavior appears. It is therefore permissible to "linearize" Eqs. (6a) and (6b) by setting $N_i=1$. It is also clear that a single polarization variable

$$P=\sum_{i=1}^{J} p_i\lambda_i P_i \Big/ \sum_{i=1}^{J} p_i^2\lambda_i$$

may be defined, together with transformed space and time variables $\mu=X$, $\tau=T-X>0$, such that Eqs. (6a) and (6b) reduce to the form

$$\frac{\partial E}{\partial \mu}=\bar{\alpha}P, \quad \frac{\partial P}{\partial \tau}=E ,$$

where $\bar{\alpha}=\alpha\sum_i p_i^2\lambda_i$.

These are the linearized equations for the corresponding nondegenerate problem and possess exact analytic solutions.[24] The solutions are easily extended where field and polarization losses are retained, by making the transformations $(P,E)\rightarrow(P,E)\exp(\kappa L\mu+\frac{1}{2}\tau_E\gamma_2\tau)$ in the equations of motion. The individual polarizations are given by

$$P_i(\mu,\tau)=P_i(\mu,0)+p_i\bar{\alpha}\tau\int_0^{\mu}d\mu' P(\mu',0)I_1(2\sqrt{\bar{\alpha}\tau(\mu-\mu')})/\sqrt{\bar{\alpha}\tau(\mu-\mu')}+p_i\int_0^{\tau}d\tau' E(0,\tau')I_0(2\sqrt{\bar{\alpha}\mu(\tau-\tau')}) ,$$

where the term containing $E(0,\tau)$ is intended to simulate the effects of zero-point fluctuations in the vacuum field, while the field amplitude is correspondingly

$$E(\mu,\tau)=\bar{\alpha}\int_0^{\mu}d\mu' P(\mu',0)I_0(2\sqrt{\bar{\alpha}\tau(\mu-\mu')}) + \bar{\alpha}\mu\int_0^{\tau}d\tau' E(0,\tau')\frac{I_1(2\sqrt{\bar{\alpha}\mu(\tau-\tau')})}{\sqrt{\bar{\alpha}\mu(\tau-\tau')}} .$$

The condition $E(\mu,0)=\bar{\alpha}\int_0^{\mu}P(\mu',0)d\mu'$ shows the interdependence of the initial field and the net initial polarization. If one of the component polarizations, say $P_k$, could be prepared with a much larger initial amplitude than the remaining components, then the shape and delay of the first emitted pulse would be determined primarily by $P_k(\mu,0)$. The quantum-mechanical treatment of the problem sketched in Appendix A, however, is consistent with our assumption and adoption of equal tipping angles for all of the degenerate transitions throughout the remainder of the paper.

The existence of fluctuations in the radiant output from many repeated experiments (manifested as variations in the delay, width, and height of the first emitted pulse) cannot affect the presence of qualitative features, i.e., internal structure, within the first pulse. Any such structure is inevitably always present owing to the early locking of the Bloch angles into their preferred ratios. In other words, statistical variations can appear in the net polarization owing to the initial uncertainty, but do not appear between the component polarizations.

## III. NUMERICAL SOLUTIONS OF THE EQUATIONS OF MOTION

As no satisfactory analytical procedures for integrating the equations of motion (1a)—(1c) are currently available, we have resorted to numerical integration on the computer, using a predictor-corrector routine. On the time scales relevant to SF the homogeneous broadening is usually ignorable, and therefore the relaxation terms have been omitted for the numerical calculations unless otherwise indicated. The profiles of the emitted field intensities have been calculated semiclassically as $I_+=|E^+(1,T)|^2$ and $I_-=|E^-(0,T)|^2$. Providing there is spatial symmetry (assuming, in particular, that $\Delta$ is independent of $X$), the intensities of the oppositely directed fields must possess identical time dependence. As in the corresponding problem with the nondegenerate system, we can define a delay time $T_D$ as the time interval from the termination of the pumping process to the appearance of the intensity peak of the first emitted pulse. The field amplitudes must experience their greatest variations at each end of the rod, and the Bloch angles $\sigma_i$ therefore will change most rapidly at the ends. The angles $\rho_i$ were observed in all cases to evolve from their initial uniform value of $\pi/4$ to the values $\pi/2$ and zero, respectively, at the opposite ends, while at the midpoint of the rod $\rho_i(\frac{1}{2},T)$ retained the value $\pi/4$ at all times. The transition to this spatial configuration was complete within, and often well before, the delay time. Designating the time for completing this transition process as $T_S$, we have found empirically that when $T>T_S$ *all of the Bloch angles* $\sigma_i$ *maintain constant ratios to each other.* In the case $J=2$ this ratio is 1:2 exactly, and hence we can write $\sigma_1=2\sigma_2$ $(=\sigma)$ and thus

$$N_1=\cos\sigma, \quad N_2=\cos(\tfrac{1}{2}\sigma) , \tag{7a}$$

$$P_1^{\pm}=\sin\sigma\times\begin{cases}\cos\rho\\ \sin\rho\end{cases}, \quad P_2^{\pm}=\sin(\tfrac{1}{2}\sigma)\times\begin{cases}\cos\rho\\ \sin\rho\end{cases} , \tag{7b}$$

$$E^{\pm}=\frac{\partial\sigma}{\partial T}\times\begin{cases}\cos\rho\\ \sin\rho\end{cases} . \tag{7c}$$

The following behavior also has been observed for $T>T_S$.

(1) The population inversions at equilibrium, which were ascertained by looking at the long-time domain and if necessary utilizing strong field damping $(\kappa L\gg 1)$ to remove long-lived ringing effects, were observed to be quite different for each species of transition. For $\Delta\ll 1$, the equilibrium values in the $Q(2)$ system are $N_1=N_{1e}=-\frac{1}{4}$, $N_2=N_{2e}=-\frac{7}{8}$.

(2) It has also been found that one effect of retaining the atomic damping terms in Eqs. (1b) and (1c) is to dampen the output field intensities exponentially, and the equilibrium values of the inversions in these circumstances then revert to $N_{1e}=N_{2e}=-1$. This shows that ultimately both of the populations must decay (e.g., by spontaneous emission) to their respective ground states.

(3) The effective angle $\sigma$ possesses *two* possible equilibrium values when $J=2$, independent of the spatial variable $X$:

$$\sigma_e^{(1)}=2\cos^{-1}N_{1e}=2\pi-\cos^{-1}N_{2e}=\delta=3.647 \text{ rad} ,$$

$$\sigma_e^{(2)}=4\pi-\delta .$$

Which of the two possible values is adopted by the system in the long-term domain depends upon the parameters $\alpha$, $\Delta$, and $\kappa L$. In the regime of SF (small $\alpha$), or if the field damping is sufficiently great, we find that the equilibrium value is always $\delta$. In the oscillatory regime (large $\alpha$) with $\Delta \ll 1$ we find for the long-time limit of $\sigma$ $(=\sigma_\infty)$

$$\sigma_\infty=\delta \text{ when } \Delta \lesssim 5\times 10^{-4} ,$$

$$\sigma_\infty=4\pi-\delta \text{ when } \Delta > 5\times 10^{-4} .$$

(4) Typical behavior of the emission profile is shown in Figs. 1(a) and 1(b). Doubly peaked pulses appear in the $J=2$ case when $\kappa L < 1$, but for $\alpha \lesssim 1$ this feature is only observed when $\Delta$ is sufficiently small [when $\sigma_i(0) > 10^{-4}$ the leading pulse can have a large trailing "wing"]. This behavior for two well-coupled dipole species in equal admixture differs from the behavior to be found (see Fig. 2) when a small proportion of one species is strongly driven by the other species (this corresponds to setting $\lambda_2 \ll \lambda_1$). If, in the equally mixed case, the damping parameter $k=\kappa L$ is allowed to gradually increase, then the trailing peak within the first emitted pulse gradually declines, eventually disappearing. Simultaneously, a second large peak emerges and grows at some distance from the first,

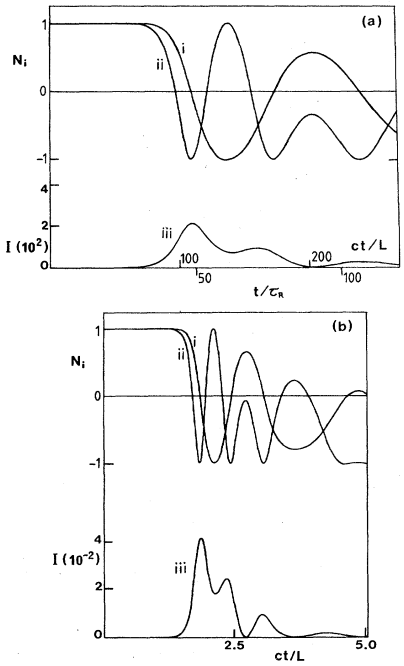


FIG. 1. (a) Time development of population inversions at the ends (i) $N_2$, (ii) $N_1$, and output intensity (iii) in the SF regime ($\tau_E=\frac{20}{3}$, $\tau_R=7.5$, $\lambda=1$, $\Delta_i=10^{-10}$, $k=0$). (b) Time development as in (a) in the OF regime ($\tau_R=0.075$, other parameters unchanged).

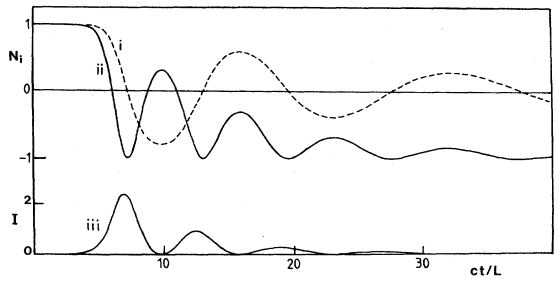


FIG. 2. Time development as in Fig. 1 for an almost nondegenerate medium ($\tau_R=0.5$, $\lambda=10^{-50}$, $\Delta_i=10^{-6}$). Broken line represents $N_2(t)$. As $t\to\infty$, $N_2\to 0$ and $N_1\to 1$.

and the ringing decreases. Examples of this behavior are shown in Figs. 3(a) and 3(b). There is an optimal value of $k$, designated $k_0$, for which the output intensity resolves into two little-ringing pulses most clearly, and whose time delays are in the approximate ratio 2:1 (the ratio has been

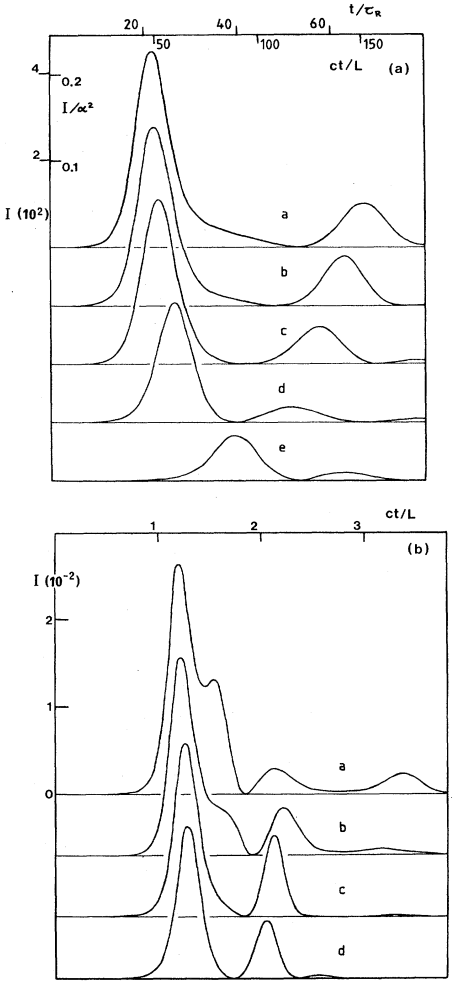


FIG. 3. (a) Output intensity in $Q(2)$-degenerate SF ($\Delta_i=10^{-6}$; $k$ is *a*, 0.0; *b*, 0.2; *c*, 0.5; *d*, 1.5; *e*, 5.0; other parameters unchanged from Fig. 1). (b) Output intensity in $Q(2)$-degenerate SF ($\Delta_i=10^{-6}$; $k$ is *a*, 0.0; *b*, 0.5; *c*, 1.0; *d*, 1.5).

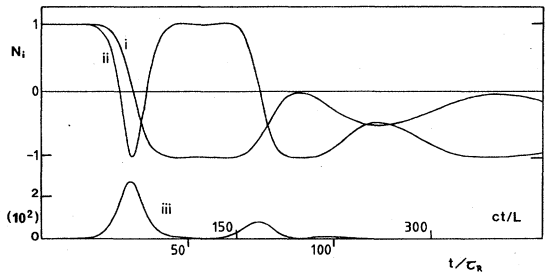


FIG. 4. Time development as in Fig. 1 in SF ($\Delta_i=10^{-7}$, $k=0.7$; other parameters unchanged).

found to vary within the range 1.7—2.4). This behavior is depicted in Fig. 4.

(5) The cumulative area $\int_0^T E^+(1,T')dT'$ at the end of the rod has been accurately measured numerically. At $k=k_0$ the net area of the first pulse (which enjoys compact support) is $2\pi$ in the $J=2$ case, while the subsequent net area (including ringing) is $\pm(2\pi-\delta)$. The total area is always $\delta$ when $\alpha\lesssim 1$ and can be either $\delta$ or $4\pi-\delta$ when $\alpha\gg 1$.

(6) The area, height, and width of the second pulse have been found to vary considerably as $\alpha$ changes, even at $k=k_0$.

(7) The optimal loss parameter for two-pulse output, $k_0$, is almost independent of $\alpha$ if $\alpha\lesssim 1$, but depends upon $\alpha$ to an increasing extent as $\alpha$ becomes larger. Both $k_0$ and the time delays to the other two major pulses depend on $\ln\Delta$. This behavior can be clearly seen in Fig. 5. The *linear* dependence of $k_0$ with respect to $\ln\Delta$ has been verified over the range of values $10^{-2}$—$10^{-15}$ for $\Delta$.

(8) Graphs of the time development of the inversions at the ends of the rod (see Fig. 4) reveal a type of in-phase beating, one against the other, which can still occur even when significant emission of energy has ceased.

(9) In addition to the existence of the stable configurations represented by the equilibrium values $\sigma_e^{(1,2)}$ discussed above, there are apparently also spatially dependent quasistable configurations in the long-term regime providing that $\Delta$ is sufficiently small and that $\alpha\gg 1$. These "kink-like" solutions for large $\alpha$ have the characteristics of the $4\pi-2\delta$ kinks which have been described in absorbing contexts.[12] They move extremely slowly on the ultrashort time scale. Their precise number and positions depend critically upon the values of $\alpha$, $k$, and $\Delta$. No evidence of their formation has been found in the superfluorescent regime, however.

(10) An inverted $Q(2)$ system with $\Delta_1=10^{-4}$ and $\Delta_2=10^{-6}$ has been found to evolve in an almost identical manner to one with $\Delta_1=\Delta_2=10^{-4}$ (a slight delay distinguishes the former from the latter case).

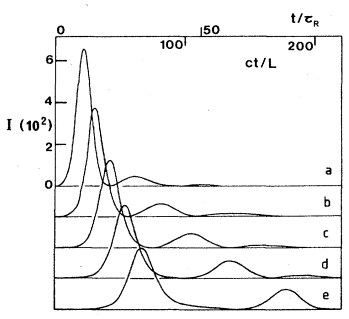


FIG. 5. Output intensity in $Q(2)$-degenerate SF ($-\log_{10}\Delta_i$ is *a*, 3; *b*, 4; *c*, 5; *d*, 6; *e*, 7; $k=0.5$; other parameters unchanged from Fig. 1).

## IV. INTERPRETATION OF RESULTS AND DISCUSSION

The stability of doubly peaked pulses of area $4\pi$ propagating within a $Q(2)$-degenerate full attenuator was predicted in 1976 (Refs. 8 and 9) and was studied experimentally.[10,11] These doubly humped pulses are basically a bound pair of $2\pi$ hyperbolic secant pulses and possess the properties of solitary waves together with, in some cases, an additional internal "wobble." Apart from the different initial and boundary conditions, the equations of motion [(1a)—(1c)] for the amplifier differ from the attenuation equations primarily in the sign of the right-hand side of Eq. (1a). It might be anticipated, therefore, that similar doubly humped pulses will occur in amplifying contexts, providing that the polarization losses are sufficiently small. In approaching this problem, we will simplify the dynamics by considering only propagation of a single field mode, as in the one-way model of SF (Refs. 21—24); compared with the two-way model the effective difference in the emission lines in the magnitude of the ringing. Using the collective Bloch angle $\sigma$ as the dynamical variable, setting $\lambda_1=1$, $\lambda_2=\lambda$, and also $\rho_i=0$, we obtain from Eqs. (1a)—(1c) and (5) a partial differential equation of the sine-Gordon type:

$$\sigma_{TT}+\sigma_{XT}+k\sigma_T=\alpha[\sin\sigma+\tfrac{1}{2}\lambda\sin(\tfrac{1}{2}\sigma)]\ . \tag{8}$$

The distortionless form of Eq. (8) taking $k=0$ is

$$(1-V^{-1})\sigma_{\eta\eta}=\alpha[\sin\sigma+\tfrac{1}{2}\lambda\sin(\tfrac{1}{2}\sigma)]\ , \tag{9}$$

where $\eta=T-X/V$, and $V=v/c$ is the field envelope velocity (scaled to the speed of light) in the dielectric. A single-pulse solution of Eq. (9) which appears to exhibit $4\pi$ solitonlike behavior requires that the condition

$$N_i(X,\pm\infty)=+1 \tag{10}$$

be fulfilled. The dynamical variables are then obtained for $\lambda=1$ as

$$E(\eta)=10\sqrt{\alpha}(1-V^{-1})^{-1/2}\operatorname{sech}\theta/(1+4\operatorname{sech}^2\theta)\ , \tag{11a}$$

$$N_2=\frac{1-6\operatorname{sech}^2\theta}{1+4\operatorname{sech}^2\theta},\quad N_1=-(2N_2^2-1)\ , \tag{11b}$$

$$P_2=2\sqrt{5}\operatorname{sech}\theta\tanh\theta/(1+4\operatorname{sech}^2\theta)\ ,$$
$$P_1=2N_2P_2\ , \tag{11c}$$

where $\theta=\frac{1}{2}[5\alpha/(1-V^{-1})]^{1/2}\eta$. The envelope velocities are greater than the velocity of light *in vacuo,* however, and therefore such pulses cannot be stable. These special solutions in terms of the single variable $\eta$ can only be physically relevant in transient situations for which prop-

agation effects are ignorable, such as might occur close to the ends of the rod. We note that Figs. 1 and 2 show similar doubly peaked leading pulses emitted from an initially inverted $Q(2)$-degenerate medium. Asymmetry appears, however, in the reduced amplitude of the second lobe of the pulse (and also in the corresponding inversion curves).

In adapting the double sine-Gordon equation (8) to the regime of pure superfluorescence we may employ the same argument as has been used in a nondegenerate context[21] which allows the term $\sigma_{TT}$ to be ignored relative to the term $\sigma_{XT}$. Undamped superfluorescence from a $Q(2)$-degenerate system is thus described by

$$\sigma_{XT}=\alpha[\sin\sigma+\tfrac{1}{2}\lambda\sin(\tfrac{1}{2}\sigma)] \tag{12}$$

and this equation clearly admits of a similarity-variable solution.[4] More generally, for a $J$-fold degeneracy, the right-hand side of Eq. (12) can be suitably modified to accommodate the $J$ terms. It should also be noted that Eq. (12) describes the propagation of a superfluorescent pulse within a $Q(2)$-degenerate amplifier,[35] albeit with very different boundary conditions. The general shape and behavior of such an amplified pulse bears resemblance to that found for the nondegenerate amplifier, as revealed by numerical integration of the similarity form of the sine-Gordon equation.[4] The important new feature of the ringing lobes is the closely coupled doublet structure within each lobe. The first peak in this structure can be interpreted in terms of cooperative emission via the strongest dipole, while stimulated emission via the weaker dipole accounts for the second peak. Defining the similarity variable to be $\psi=2(\alpha XT)^{1/2}$, we find that Eq. (12) becomes the ordinary differential equation

$$\sigma_{\psi\psi}+\psi^{-1}\sigma_{\psi}=\sin\sigma+\tfrac{1}{2}\lambda\sin(\tfrac{1}{2}\sigma)\ . \tag{13}$$

The second term $\psi^{-1}\sigma_{\psi}$ in Eq. (13) can be regarded as a (variable) damping effect which introduces asymmetry in the doubly humped solutions of

$$\sigma_{\psi\psi}=\sin\sigma+\tfrac{1}{2}\lambda\sin(\tfrac{1}{2}\sigma)\ . \tag{14}$$

Amplifying solutions of the latter equation admit ringing, expressible generally in terms of Jacobi elliptic functions, and the field amplitudes $\sigma_T$ propagate at speeds less than $c$ [note that unphysical periodic solutions of the distortionless equation (9) also exist, in addition to the single-pulse hyperbolic profiles; in these cases the speeds are greater than $c$]. The two differential equations (9) and (13) thus may be regarded as representing extreme limits of behavior, and the undamped solutions of their common parent, Eq. (8), will exhibit a wide range of behavior within these limits.

A very useful device for interpreting many of the dynamical features of this type of system is to construct a diagram of the potential-energy function $U(\sigma)=\sum_{i=1}^{J}N_i(\sigma)$, where $\sigma$ is the collective Bloch angle. Figure 6 depicts this function for the cases $J=2$ and 3. Examining the $J=2$ case first, we see that the doubly humped shape of $E(\eta)$ corresponds with the profile of the function $U(\sigma)$ over the range $(2\Delta)^{1/2}\leq\sigma\leq 4\pi-(2\Delta)^{1/2}$; thus the two peaks are associated with the presence of two

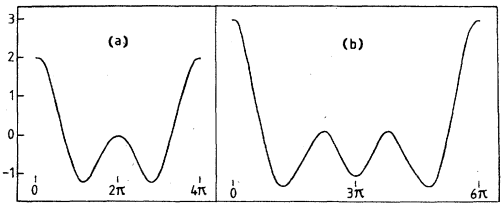


FIG. 6. Potential energy of the atoms $U$ as a function of the Bloch angle $\sigma$ for the degeneracies (a) $J=2$, (b) $J=3$.

energy wells, and it can be anticipated that energy losses will introduce asymmetries in $E(\eta)$. A helpful analogy is the dynamical problem of a particle of unit mass, suitably damped and constrained to move from an initial position of rest within a potential well of shape $U(y)=\alpha(\cos y+\lambda\cos\frac{1}{2}y)$. With linear damping $k\dot{y}$ present as well, the equation of motion is

$$\ddot{y}+k\dot{y}=-\partial U/\partial y\ . \tag{15}$$

Depending upon the value of the damping constant $k$, the system may come to rest at either of the two minima or could conceivably come to rest in the metastable position at $y=2\pi$. The latter situation occurs when $k$ possesses the exact value $k_0$ given by

$$k_0=\tfrac{1}{4}\lambda\alpha^{1/2} \tag{16}$$

and corresponds to a fission of Eq. (15) into two equivalent parts, with the solution

$$\sin(\tfrac{1}{2}y)=\operatorname{sech}[\alpha^{1/2}(T-T_D)]\ . \tag{17}$$

Assuming for the initial condition $y_0=y(0)\ll\pi$, we have the corresponding delay time as

$$T_D=\alpha^{1/2}\ln(4/y_0)\ . \tag{18}$$

In Figs. 7(a) and 7(b) we see $y$ and $\dot{y}$ versus time for $k=0$ and $k\simeq k_0$, illustrating the above points as well as other features of the problem.

The damped sine-Gordon equation (8) differs from the simpler equation (15) by its particular dependence upon both time and space variables, $T$ and $X$. Once again, however, there is a special solution of Eq. (8) in terms of the variable $\eta=T-X/V$ which exhibits solitary-wave-like properties. We assume that there is a special value of $k$ $(=\kappa L)$ which allows Eq. (8) to split into equivalent parts and which again will be designated $k_0$. With this assumption, we find

$$\sigma_{\eta\eta}=(1-V^{-1})^{-1}\sin\sigma,\quad \sigma_{\eta}=\frac{\lambda\alpha}{2k_0}\sin(\tfrac{1}{2}\sigma) \tag{19}$$

from which we immediately infer that the velocity $V$ of the field amplitude within the medium has the value

$$V=[1-(4k_0\lambda^{-1})^2/\alpha]^{-1}\ , \tag{20}$$

In Fig. 8 the magnitude of the velocity $V$ is shown as a function of $\alpha$; $V$ is always negative, implying that the interior field profile travels in the opposite direction to the emitted pulse, as it must. Superfluorescent behavior occurs within the domain $|V|<1$ while the regime of os-

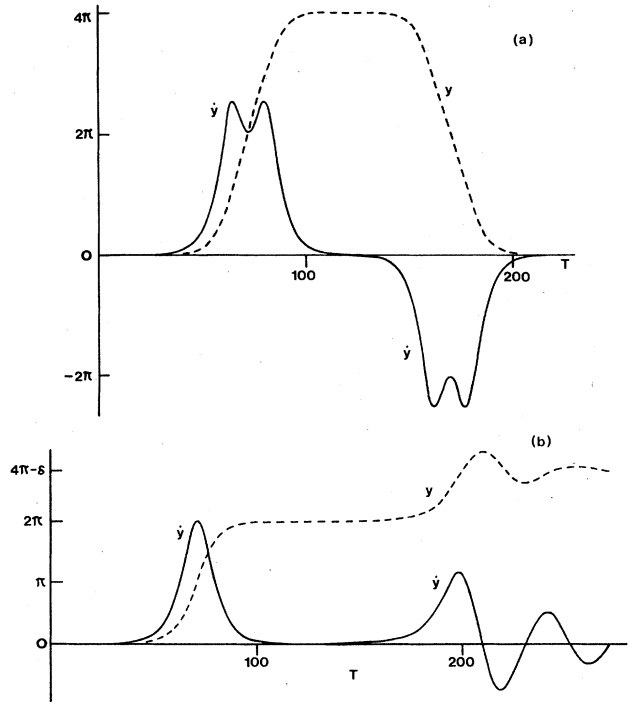


FIG. 7. (a) Solutions $y(t)$ and $\dot{y}(t)$ of $\ddot{y}=10[\sin y+\frac{1}{2}\sin(\frac{1}{2}y)]$. (b) Solutions $y(t)$ and $\dot{y}(t)$ of $\ddot{y}+k\dot{y}=10[\sin y+\frac{1}{2}\sin(\frac{1}{2}y)]$ when $k=0.7905$ (which differs from $k_0=\frac{1}{4}\sqrt{10}$ by 0.01%).

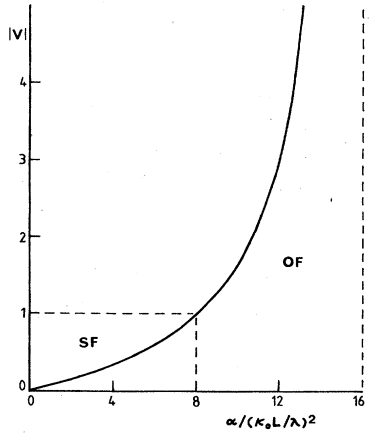


FIG. 8. Velocity of the interior field profile, when $k=k_0$, as a function of $\alpha\lambda^2/k_0^2$.

cillating fluorescence corresponds with $|V|>1$. The analytic solutions for the dynamical variables in this situation are easily found. At the end of the rod ($X=1$) we obtain the time-dependent quantities

$$N_1=-\cos\sigma=1-2\tanh^2\phi\ , \tag{21a}$$

$$N_2=\cos(\tfrac{1}{2}\sigma)=-\tanh\phi\ , \tag{21b}$$

$$P_1=\sin\sigma=-2\tanh\phi\,\mathrm{sech}\phi\ , \tag{21c}$$

$$P_2=\sin(\tfrac{1}{2}\sigma)=\mathrm{sech}\phi\ , \tag{21d}$$

$$E=\frac{\sigma}{2k_0}\mathrm{sech}\phi\ , \tag{21e}$$

where

$$\phi(T)=\frac{\lambda\alpha}{4k_0}(T-T_D)\ . \tag{22}$$

These special solutions can generate amplitude profiles which propagate in free space as $2\pi$ pulses, which can be verified by evaluating the area $\int_{-\infty}^{\infty}E\,dt$. Although such pulses are unstable in the context of propagation *within* an amplifier (i.e., they distort rapidly), it can be inferred that the solitary solution of Eq. (19) in terms of $\eta$ is sufficiently stable near the end of the medium for its motion to control the behavior of the transmission.

A general solution of Eq. (8) for initial and boundary conditions appropriate to SF emission has not been found and is presumably a complicated function of $X$ and $T$; however, the above solution of the end of the rod possesses all of the properties that have been obtained with $k=k_0$ in the numerical computations. It can be inferred that the assumed special value $k=k_0$ allows the linear (small-angle) solution for $\sigma(T)$ to evolve from the first form of $\theta=2[(1+\frac{1}{4}\lambda)\alpha(T-1)]^{1/2}$, namely

$$\sigma(T)\sim\sigma_0(2\pi\theta)^{-1/2}e^{\theta-k_0},\quad X=1 \tag{23}$$

into the second form obtained as the small-angle limit of Eq. (21c)

$$\sigma(T)\sim 4e^{-\phi(T)},\quad X=1 \tag{24}$$

within a time $T_1$ much smaller than the delay time $T_D$. Further discussion of the first linear solution, Eq. (23), is given in Appendix B. In support of the above interpretation of the "$2\pi$ behavior" which has been generated in the numerical solutions, we note first that a reconciliation of the two expressions (23) and (24) implies that $k_0$ varies approximately linearly with respect to $-\ln\sigma_0$. We also observe that Eq. (23) implies that $T_D$ is approximately proportional to $\alpha^{-1}(\ln\sigma_0)^2$ in the SF regime. The latter result depends crucially upon the validity of extrapolating the linear solution (23) for $\sigma(T)$ to the delay time $T_D$ (i.e., to $\sigma\sim\pi$). For the oscillating fluorescence regime, however, only the second linear form (24) may be validly extrapolating (even crudely) to $T=T_D$. In this case the transition time $T_1$ is small enough to ensure that the angle $\sigma$ has increased from $\sigma_0$ by less than an order of magnitude at $T=T_1$; assuming $k_0$ proportional to $\alpha^{1/2}$, we therefore infer that the delay time in the oscillating fluorescence regime is proportional to $\alpha^{-1/2}|\ln\sigma_0|$. These various predictions have all been borne out by a systematic empirical analysis of the computed field intensities. Small corrections to $k_0$ and the delay time are required, however, when these results predicted for the one-way propagating model are compared with the corresponding computed results using counterpropagating fields. The numerical results have also revealed the following parameter dependence of $k_0$:

$$k_0=A(\alpha)-B(\alpha)\ln(\sigma_0/\sqrt{2})\ , \tag{25}$$

where the parameters $A(\alpha)$ and $B(\alpha)$ possess the limiting behavior (a) for SF ($A=0$, $B=B_1$) and (b) for OF ($A=\frac{1}{4}\lambda\alpha^{1/2}$, $B=B_2<B_1$, in which $B_1$ and $B_2$ are different constants).

It is appropriate at this stage to reintroduce statistical considerations. The characteristic field loss parameter $k_0$ depends upon $\sigma_0$, where $\sigma_0$ represents a statistical average associated with uncertainty in the initial polarization. The actual value of $k_0$ in a given experimental situation could be determined by performing a large number of measurements of output profiles and delays for a given value of $k$, from which a probability that $k=k_0$ could be determined by simply observing the proportion of pulse pairs which are "well separated." This probability could then be determined as a function of $k$ (e.g., $k$ might be varied by altering both $L$ and $n$ in such a way that $\alpha$ remains constant). Presumably the value of $k$ corresponding to the probability maximum is $k_0$. Such an experiment could also be simulated numerically, using a fluctuating polarization source. The fluctuations in the time delay of a well-separated second pulse of area $2\pi-\delta$ would be complicated by the additional statistics attached to the unstable equilibrium phase during which $N_1\simeq 1$ and $N_2\simeq -1$.

Other solutions of Eq. (8) have been studied[14] in connection with an analysis of pulse propagation within a $Q(J)$-degenerate amplifier. In this case the damping constant may be sufficiently large to ensure that the term $\sigma_{TT}\pm\sigma_{XT}$ rapidly approaches zero, and the resulting steady-state pulses must then travel at light velocity. Ringing is completely absent in this situation. The field intensity for $J=2$ is

$$I(\eta)=\sigma_\eta^2=\left[\frac{2\sigma}{\kappa L}\right]^2(1-u^2)(u+\tfrac{1}{4}\lambda)^2\,,\qquad u=\cos(\tfrac{1}{2}\sigma) \tag{26}$$

revealing two solutions.

(a) A pulse solution exists within the domain $1\geq u\geq -\frac{1}{4}\lambda$ possessing area $\delta$.

(b) A pulse solution also exists within domain $-\frac{1}{4}\lambda\geq u\geq -1$ and has area $2\pi-\delta$ (we are here assuming that $\lambda<4$). In principle, these solutions also describe radiant emission from a heavily damped rod containing inverted $Q(2)$-degenerate atoms.

## V. SUMMARY AND CONCLUSIONS

Radiative emission from both ends of an extended medium whose atoms possess the simplest type of hyperfine degeneracy [$Q(J)$ symmetric, where $J$ is an integer] has been investigated in terms of a simple one-dimensional model, on the assumption that the initial pumping process populates all upper hyperfine levels equally. Numerical results for the temporal and spatial evolution of an inverted $J=2$ system reveal qualitative differences from the nondegenerate ($J=1$) case, within both the regimes of superfluorescence and oscillating fluorescence. Analytic results have been obtained only for a simplified model in which the propagation of energy is unidirectional. For $J=2$ the atoms possess two dipole matrix elements in the ratio 1:2. The one-way Maxwell-Bloch theory for the superfluorescent regime then yields, in terms of the collective Bloch angle $\sigma(X,t)$, an underlying equation of motion sometimes described as the double sine-Gordon equation. Two important features are an amplifying state occurring at $\sigma=\pi$ (which is unstable with respect to fluctuations) and two attenuating equilibrium states of lower energy at $\sigma=\delta$ and $4\pi-\delta$, where $\delta=2\cos^{-1}(-\frac{1}{4})$. Depending upon the scale of the dissipative processes (simulated in our model by the insertion of a linear term $k\dot{\sigma}$ into the equation of motion), the emission will be either a doubly peaked (or asymmetric) pulse together with substantial ringing (for $k\ll k_0$, where $k_0$ is a characteristic solution parameter) or alternatively two well-separated simple pulses with minimal ringing ($k\sim k_0$). The observation of the latter emission state will be complicated by statistical processes, however. More complicated behavior is indicated when $J>2$.

## ACKNOWLEDGMENTS

The author is grateful to R. K. Bullough for informative and constructive conversations on the subject of superfluorescence. Large sections of the work reported herein were accomplished during periods spent at Institute of Science and Technology, University of Manchester (UMIST), Manchester, and at Imperial College of Science and Technology, University of London, London.

## APPENDIX A

The equations derived semiclassically in Sec. II are basically the same as their quantum-mechanical counterparts, owing to the linearity of the early stages of the dynamical evolution. The main differences are that the quantum-mechanical theory treats both the polarizations $P$ and the field amplitude $E$ as Bose operators in the linear regime:[34]

$$[P_i^\dagger(\mu,\tau),P_i(\mu',\tau)]\simeq\frac{4}{N}\delta(\mu-\mu')\,, \tag{A1a}$$

$$[E(\mu,\tau),E^\dagger(\mu,\tau')]\simeq\frac{4}{N}\delta(\tau-\tau')\,. \tag{A1b}$$

These become exact identities where $\tau=0$ in Eq. (A1a) and $\mu=0$ in Eq. (A1b). In the semiclassical theory, $E(\mu,0)$ and $E(0,\tau)$ can be given small values consistent with fluctuations in the vacuum field and in the initial polarization field. The more restricted semiclassical initial and boundary conditions (2) and (3) are strictly not compatible with the solutions for $E(\mu,\tau)$ and $P(\mu,\tau)$ given in Sec. II, unless it can be held that $P(\mu,0)$ can be finite together with $\int_0^\mu P(\mu',0)d\mu'=0$.

Since $P_i$ and $P_i^\dagger$ correspond approximately with atomic lowering and raising operators, respectively, it is possible to calculate the atomic initial state averages:

$$\langle\uparrow|P_i^\dagger(\mu,0)P_i(\mu',0)|\uparrow\rangle=\frac{4}{N}\delta(\mu-\mu')\,. \tag{A2}$$

If the degeneracy is manifested only within each atom (that is, all $\lambda_i=1$), then we also find

$$\langle \uparrow P^{\dagger}(\mu,0)P(\mu',0) \mid \uparrow \rangle = \frac{\sum_i p_i^2 \langle \uparrow \mid P_i^{\dagger}(\mu,0)P_i(\mu',0) \mid \uparrow \rangle}{\sum_i p_i^2} = \frac{4}{N}\delta(\mu-\mu') \ . \tag{A3}$$

The buildup of field intensity within the linear regime is thus

$$I(\mu,\tau) = \langle \text{vac},\uparrow \mid E(\mu,\tau)E^{\dagger}(\mu,\tau) \mid \uparrow,\text{vac} \rangle = \frac{4\bar{\alpha}^2}{N}\int_0^{\mu} I_0^2(2\sqrt{\bar{\alpha}\mu'\tau})d\mu' = \frac{4\bar{\alpha}^2}{N}\{I_0^2(\theta)-I_1^2(\theta)\}$$

with $\theta^2 = 4\bar{\alpha}\tau\mu$.

## APPENDIX B

The linear solution of the differential equation for $\sigma(X,T)$ at $X=1$ has been given for the regime in which $\theta \gg 1$, where $\theta = 2[(1+\frac{1}{4}\lambda)\alpha(T-1)]^{1/2}$ [see Eq. (23)]. In order to arrive at this result, it has been found necessary to consider the full linear solution of the Maxwell-Bloch equations with the inclusion of a field-loss term. This problem has already been analyzed in detail in Ref. 24, and we may borrow the relevant results here. With $\beta = (1+\frac{1}{4}\lambda)\alpha$ and the obvious assumption $T \gg X$, we find for the full linear result the alternative but equivalent expressions

$$\sigma(X,T) = \sigma_0\left[1+2\sqrt{\beta T}\int_0^{\sqrt{X}} e^{-ku^2} I_1(2\sqrt{\beta T X u})du\right] \tag{B1}$$

$$= \sigma_0\left[e^{-kX} I_0(2\sqrt{\beta T X}) + e^{\beta T/k}[1-J(kX,\beta T/k)]\right] , \tag{B2}$$

where $I_{0,1}(\psi)$ are the modified Bessel functions of order zero and one, respectively, and $J(u,v)$ are the functions defined by

$$J(u,v) = 1 - e^{-v}\int_0^u e^{-z} I_0(2\sqrt{vz})dz \ . \tag{B3}$$

Some important properties of the functions (B3) have been listed in Ref. 24, and other properties of interest are given by Luke[36] as well as by Goldstein.[37] Note that when $k=0$ the expressions simply reduce to $\sigma = \sigma_0 I_0(2\sqrt{\beta T X})$. An analysis of the magnitudes of the terms of Eq. (B2) for the regime where $\theta \gg 1$ reveals that the first term is dominant. Using the well-known asymptotic behavior for large $\theta$, $I_n(\theta) \to (2\pi\theta)^{-1/2} e^{\theta}$, we have

$$\sigma(X,T) \to \sigma_0 (2\pi\theta)^{-1/2} e^{\theta - kX} \quad \text{as} \quad \theta \to \infty \ . \tag{B4}$$


[1] C. K. Rhodes, A. Szöke, and A. Javan, Phys. Rev. Lett. **21**, 1151 (1968).
[2] S. L. McCall and E. L. Hahn, Phys. Rev. **183**, 457 (1969).
[3] F. A. Hopf, C. K. Rodes, and A. Szöke, Phys. Rev. B **1**, 2883 (1970).
[4] G. L. Lamb, Jr., Rev. Mod. Phys. **43**, 99 (1971).
[5] I. A. Poluektov, Yu. M. Popov, and V. S. Roitberg, Kvant. Elektron. (Moscow) **1**, 1309 (1974) [Sov. J. Quantum Electron. **4**, 719 (1974)].
[6] G. J. Salamo, H. M. Gibbs, and G. G. Churchill, Phys. Rev. Lett. **33**, 273 (1974).
[7] G. J. Salamo, Ph.D. thesis, The City University of New York, 1974.
[8] S. Duckworth, R. K. Bullough, P. J. Caudrey, and J. D. Gibbon, Phys. Lett. **57A**, 19 (1976).
[9] S. Duckworth, Ph.D. thesis, University of Manchester, U.K., 1976.
[10] B. Bölger, L. Beade, and H. M. Gibbs, Opt. Commun. **18**, 67 (1976).
[11] R. K. Bullough, P. J. Caudry, J. D. Gibbon, S. Duckworth, H. M. Gibbs, B. Bölger, and L. Baede, Opt. Commun. **18**, 200 (1976).
[12] R. K. Bullough, P. J. Caudry, and H. M. Gibbs, in *Solitons*, edited by R. K. Bullough and P. J. Caudrey (Springer, Berlin, 1980), p. 107, and references therein.
[13] J. A. Hermann and R. K. Bullough, from the Tenth International Quantum Electronics Conference, Atlanta, Georgia, 1978 [J. Opt. Soc. Am. **68**, 701 (1978)].
[14] J. A. Hermann, Phys. Lett. **67A**, 253 (1978).
[15] R. Friedberg and S. R. Hartmann, Phys. Lett. **38A**, 227 (1972).
[16] N. Skribanowitz, I. P. Herman, J. C. MacGillivray, and M. S. Feld, Phys. Rev. Lett. **30**, 309 (1973).
[17] J. C. MacGillivray and M. S. Feld, Phys. Rev. A **14**, 1169 (1976).
[18] J. C. MacGillivray and M. S. Feld, Appl. Phys. Lett. **31**, 74 (1977).
[19] J. C. MacGillivray and M. S. Feld, Phys. Rev. A **23**, 1334 (1981).
[20] R. Saunders, S. S. Hassan, and R. K. Bullough, J. Phys. A **9**, 1725 (1976).
[21] R. Saunders and R. K. Bullough, in *Cooperative Effects in Matter and Radiation*, edited by C. M. Bowden, D. W. Howgate, and H. R. Robl (Plenum, New York, 1977).
[22] J. A. Hermann, Phys. Lett. **69A**, 316 (1979).
[23] J. A. Hermann and R. K. Bullough, Opt. Commun. **31**, 219

(1979).
[24]J. A. Hermann, J. Phys. A **13**, 3543 (1980).
[25]R. Bonifacio and L. A. Lugiato, Phys. Rev. A **11**, 1507 (1975).
[26]R. Bonifacio and L. A. Lugiato, Phys. Rev. A **12**, 587 (1975).
[27]K. Ikeda and S. Sawada, Phys. Lett. **59A**, 205 (1976).
[28]F. Haake and R. Glauber, Phys. Lett. **68A**, 29 (1978).
[29]F. Haake, H. King, G. Schröder, J. Haus, and R. Glauber, Phys. Rev. A **20**, 2047 (1979).
[30]Q. H. F. Vrehen, H. M. J. Hikspoors, and H. M. Gibbs, Phys. Rev. Lett. **38**, 764 (1977).
[31]D. Polder, M. F. H. Schuurmans, and Q. H. F. Vrehen, J. Opt. Soc. Am. **68**, 699 (1978).
[32]M. F. H. Schuurmans and D. Polder, Phys. Lett. **72A**, 306 (1979).
[33]H. M. Gibbs, Q. H. F. Vrehen, and H. M. J. Hikspoors, Phys. Rev. Lett. **39**, 547 (1977).
[34]Q. H. F. Vrehen and M. H. F. Schuurmans, Phys. Rev. Lett. **42**, 224 (1979).
[35]I. R. Gabitov and S. V. Manakov, Phys. Rev. Lett. **50**, 495 (1983).
[36]Y. Luke, *Integrals of Bessel Functions* (McGraw-Hill, New York, 1962), p. 271.
[37]S. Goldstein, Proc. R. Soc. London, Ser. A **219**, 151 (1953); **219**, 171 (1953).